A SIMPLE EPIDEMIC MODEL WITH SURPRISING DYNAMICS

Faina Berezovsky

Mathematical Department
Howard University, Washington D.C. 20059

Georgy Karev

National Center for Biotechnology Information
National Institute of Health, Bethesda, MD 20894

Baojun Song

Department of Mathematical Sciences
Montclair State University, Upper Montclair, NJ 07043

Carlos Castillo-Chavez

Department of Mathematics and Statistics
Arizona State University, Tempe, AZ 85287-1804

(Communicated by Yang Kuang)

Abstract. A simple model incorporating demographic and epidemiological processes is explored. Four re-parameterized quantities the basic demographic reproductive number ($\mathcal{R}_d$), the basic epidemiological reproductive number ($\mathcal{R}_0$), the ratio (ν) between the average life spans of susceptible and infective class, and the relative fecundity of infectives (θ), are utilized in qualitative analysis. Mathematically, non-analytic vector fields are handled by blow-up transformations to carry out a complete and global dynamical analysis. A family of homoclinics is found, suggesting that a disease outbreak would be ignited by a tiny number of infectious individuals.

1. **Introduction.** There is a long history of application of dynamical systems to epidemiology beginning with the work of Ross (1911). Research in theoretical and mathematical epidemiology has expanded ever since (see Busenberg and Cooke (1983), Anderson and May (1991), Hethcote (1999), Aparacio, Capurro and Castillo-Chavez (2000), Brauer and Castillo-Chavez (2001), and Castillo-Chavez et al. (2002a, 2002b)). The mathematical theory of epidemic models took off in the 1970s, when a large number of mathematicians involved in mathematical biology. The approach was based on the work of Kermack and MacKendrick (1927, 1932), two students of Ross, and on extensions of the work on vector-transmitted diseases by Ross himself (1911). The work of Lajmanovich and Yorke (1976) on "general" SIS multi-group models implied that general epidemic models were "robust" and in some sense suggested that epidemics could be well understood. A basis for this degree of optimism came from the fact that Lajmanovich and Yorke's work (1976) suggested "general" epidemiological models could be written as monotone systems

where there is a simplifying rich theory. The general feeling at that time (and still to some degree today) was that the spectral radius of the next generation operator (Diekmann and Heesterbeek (2000)) associated with the differential equations that modeled the epidemic completely characterized the dynamics. The qualitative dynamics of "general" epidemic models were reduced to the existence of a threshold (spectral radius or basic reproductive number) that determines the stability and existence of non-trivial equilibria.

The basic reproductive number $\mathcal{R}_0$ gives the average number of secondary cases of infection generated by an initially tiny population of infectious individuals in a population of mostly susceptibles. The basic reproductive number $\mathcal{R}_0 < 1$ implies that the initial set of infectious individuals will not be able to replace themselves before they die or recover and, consequently, the disease will not be able to successfully spread or invade. In other words, the infectious-free state, an equilibrium typically supported by epidemic models, is locally asymptotically stable. However, this infectious free-state loses its local stability whenever $\mathcal{R}_0 > 1$. In fact, $\mathcal{R}_0 > 1$ "typically" signals the birth of a locally asymptotically stable endemic state where the disease is always present. For many epidemiological systems it has been shown that the local stability of these states is actually a global property. In other words, $\mathcal{R}_0 = 1$ is the "tipping" point (threshold) that determines the existence and stability of the endemic state. That is, often the dynamics are characterized by a global transcritical bifurcation (see Hethcote (1999)).

However, the dynamics described above (global transcritical bifurcation) are not generic but often the result of constrained dynamics. Most models assumed that the population in question was constant. Multi-population models assumed that each subpopulation also had a fixed number of individuals (Hethcote and Yorke (1984)). Initial efforts to help in understanding the dynamics of HIV epidemics naturally weakened these assumptions (see Castillo-Chavez (1988, 1989)). The removal of these assumptions resulted (when appropriate) in more realistic epidemic models with richer dynamics. For example, these systems have been shown to support multiple equilibria and, in the process, raised some questions on the usefulness of $\mathcal{R}_0$ (see Hadeler and Castillo-Chavez (1995), Feng et al. (2000), and van den Driessche et al. (2002)).

The study of models with variable population size (which began in the early 1980s) due to demographic processes also illustrated the possibility of richer dynamics (see Hethcote (1999)). In the context of models with variable population size, the view that the qualitative dynamics of such systems are controlled in specific ways by two thresholds began to emerge. The first threshold is a demographic threshold $\mathcal{R}_d$, the basic reproductive number for the demographic process. Basically, $\mathcal{R}_d > 1$ implies that each founder individual (initially small population) leaves more than one descendant on average before it dies. In this case the population grows and prospers; that is, a critical mass of individuals for the disease to spread may be supported. On the other hand, $\mathcal{R}_d < 1$ implies that the population will not survive (births will exceed deaths at the beginning of the process); that is, no critical mass of individuals may be supported for the disease to spread. The second threshold is the basic reproductive number $\mathcal{R}_0$ for the epidemiological process. The processes (demographic and epidemiological) become coupled typically from the effect a disease has on demography (disease-induced mortality). The "typical" outcomes (see Hethcote (1999)) are as expected. For example, if the population initially grows at least as fast as the disease ($\mathcal{R}_d > 1$), then the disease will either

die out if $\mathcal{R}_0 < 1$, or invade the population if $\mathcal{R}_0 > 1$; and the proportion of diseased individuals may either reach a fixed level or vanish (see next section and for a detailed cases see Song et al. (2002a, 2002b), Heiderich, Huang and Castillo-Chavez (2002)). The work in this paper will exhibit additional possibilities.

Ecological models of predator-prey or parasite-host interactions and epidemiological models share the same framework of modeling. For example, Hwang and Kuang (2003) proposed the following ratio-dependent model of parasite-host interactions for experimental epidemiology in a special case of $m = 0$:

$$\begin{cases} \frac{dX}{dt} = r(X + \theta Y)(1 - c(X + Y)) - (\mu + m)X - \beta\frac{XY}{X+Y}, \\ \frac{dY}{dt} = -(\mu + d)Y + \beta\frac{XY}{X+Y}. \end{cases} \tag{1.1}$$

Here $X(t)$ and $Y(t)$ represent respectively the densities of uninfected (susceptible) and infected hosts at time t; r is the maximum per-capita birth rate of uninfected hosts; c measures the per-capita density-dependent reduction in birth rate ($1/c$ is also called the carrying capacity if $c \neq 0$); β denotes the transmission rate (the infection rate constant); μ is the natural mortality; θ is the relative fecundity of infected host population, certainly $0 \leq \theta \leq 1$; d denotes the disease-induced mortality; m is the per-capita emigration rate of uninfective that is not incorporated in the original version of 1.1.

In the case $m = 0$ of model (1.1) Hwang and Kuang (2003) studied it as a parasite-host model. Because system (1.1) is not analytical at the origin, it possesses some non-trivial and very important peculiarities of dynamics. In the work by Hwang and Kuang (2003), model (1.1) was reduced by a single Briot-Bouquet (blowing-up) transformation to a Gause-type model, and was completely investigated. We show here that this Gause-type model is not equivalent to the initial model. As a result, the investigation of model (1.1) at $m = 0$ in the previous work was incomplete. Specifically, the existence of the most interesting elliptic sector (a family of homoclinic orbits of the origin that are tangent to the x-axis) was missed. The problem of analysis of the complicated singular point at the origin arises in many ratio-dependent models and can be completely solved by two blowing-up transformations, as was done, for example, by Berezovskaya et al. (2001).

Our model explored mathematically in this paper is a version of model (1.1) for $m \geq 0$ and $\theta = 1$. A partial aim of our work is to present a complete investigation of the model and to construct its phase-parameter portraits. We organize the paper as follows: Section 2 introduces the basic model and provides some basic rescaling of the system suitable for the further interpretations; section 3 studies equilibria by the normal linearization approach; section 4 focuses on the topological structure of trajectories around a particular equilibrium; in section 5 we present the phase-parameter portraits of the model; section 6 gives the analysis of model (1.1) dependently on parameter θ based on the investigation of the complicated equilibrium at the origin; section 7 contains discussion and conclusions; finally, proofs of some mathematical statements are given in the Appendix.

2. Model equations and primary results.

2.1. **Model equations.** In this paper, using as *simple* model as possible, it is shown that the dynamics of epidemic models could be richer and unpredictable.

We introduce our model through the incorporation of variable population, disease-induced mortality, and emigration into the classic model of Kermak and McKendrick (1927). The total population (N) is divided into two groups, susceptible
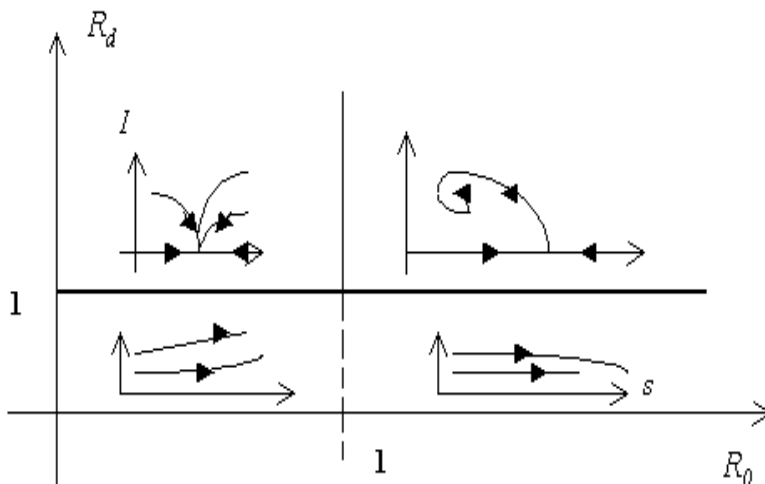
FIGURE 1. Schematic parameter-phase portrait of the model (2.1) with constant population size N.

(S) and infectious (I). The model describing the relations between the state variables is

$$\begin{cases} \frac{dS}{dt} = rN\left(1 - \frac{N}{K}\right) - \beta S \frac{I}{N} - (\mu + m)S, \\ \frac{dI}{dt} = \beta S \frac{I}{N} - (\mu + d)I, \end{cases} \tag{2.1}$$

where $N = S + I$ is the total population size; the birth process incorporates density-dependent effects through a logistic equation with the intrinsic growth rate r and the carrying capacity K; and other parameters have the same meaning as in model (1.1). Note that the growth rate of susceptibles is proportional to the total number of infectious and susceptibles, so that infectious individuals (as well as susceptibles) produce healthy susceptible offsprings.

If the disease is not present ($I = 0$), then model (2.1) reduces to the demographic equation

$$\frac{dN}{dt} = rN\left(1 - \frac{N}{K}\right) - (\mu + m)N.$$

This leads to the concepts of the basic demographic reproductive number $\mathcal{R}_d$, which is given by

$$\mathcal{R}_d = \frac{r}{\mu + m}.$$

It can be shown that if $\mathcal{R}_d > 1$, the population grows while $\mathcal{R}_d \leq 1$ implies that the population does not survive. The question of the successful invasion of the disease is determined by the linearization of (2.1) around the infection-free state: that is, around the equilibrium $((1 - \mathcal{R}_d^{-1})K, 0)$ which exists whenever $\mathcal{R}_d > 1$.

The epidemic threshold, the basic reproductive number, is then computed as

$$\mathcal{R}_0 = \frac{\beta}{\mu + d}.$$

Usually the disease will successfully invade when $\mathcal{R}_0 > 1$ but will die out if $\mathcal{R}_0 \leq 1$.

If assuming constant population, the per-capita birth rate $\Lambda = rN(1 - N/K)$ is a constant as we have seen in a number of epidemic models. Model (2.1) then has the infection-free equilibrium $A(K(1 - \mathcal{R}_d^{-1}), 0)$ for $\mathcal{R}_d > 1$ and the endemic equilibrium

$C(N\mathcal{R}_0^{-1}, N(1 - \mathcal{R}_0^{-1}))$ for $\mathcal{R}_0 > 1$. The equilibrium A is globally asymptotically stable when $\mathcal{R}_0 \leq 1$ and the endemic C is globally asymptotically stable when $\mathcal{R}_0 > 1$ (see Fig. 1). However, model (2.1) with variable population size N can support an additional infection-free state, namely $(0,0)$. (We can continuously extend the vector field of (2.1) to the origin.) The consideration of the dynamics near this state leads to somewhat surprising results.

2.2. **Rescaling and primary results.** Rescaling the model (2.1) by letting

$$x = S/K, \quad y = I/K, \qquad \text{and} \quad t = \tau/(\mu + d)$$

leads to the rescaled system

$$\begin{cases} \frac{dx}{d\tau} = \nu\mathcal{R}_d(x + y)\left(1 - (x + y)\right) - \mathcal{R}_0 \frac{xy}{x+y} - \nu x \equiv P(x, y), \\ \frac{dy}{d\tau} = \mathcal{R}_0 \frac{xy}{x+y} - y \equiv Q(x, y), \end{cases} \tag{2.2}$$

where $\mathcal{R}_0 = \beta/(\mu + d)$, $\mathcal{R}_d = r/(\mu + m)$, and $\nu = (\mu + m)/(\mu + d)$. We proceed to study the qualitative behavior of model (2.2) as a function of parameters. The goal is to construct the phase-parameter portrait of system (2.2); that is, to divide the parameter space into domains of qualitatively (topologically) different phase behaviors. Though there are three parameters in model (2.2), we pay the most attention to the dependence of qualitative peculiarities of the model solutions on the epidemiological parameter $\mathcal{R}_0$ and demographic parameter $\mathcal{R}_d$ under different levels of the *new* parameter ν defined by the ratio of the average lifespan of susceptibles to that of infections. Biologically, the feasible domain for model (2.2) is the triangular region inside $\mathbb{R}_2^+$

$$\Omega = \left\{(x, y) \in \mathbb{R}_2^+ : 0 \leq x + y \leq 1\right\}.$$

By examining the directions of vector field of system (2.2) on the boundary of Ω, we can verify that Ω is positive invariant. Furthermore, if we assume that $x(t) + y(t) > 1$ with $x(0) + y(0) > 1$ is true for all $t > 0$, then

$$\frac{d(x + y)}{dt} = \nu\mathcal{R}_d(x + y)\left(1 - (x + y)\right) - \nu x - y \leq -\alpha(x + y), \tag{2.3}$$

where $\alpha = \min\{1, \nu\} > 0$. It follows from (2.3) that $x + y$ approaches zero as $t \to \infty$, which contradicts the assumption $x + y > 1$ for all $t > 0$. We, in fact, have shown the following result.

LEMMA 1. *Any trajectory of system (2.2) starting within $\mathbb{R}_2^+$ but outside Ω will enter into Ω in a finite time.*

Hence, not only is Ω positive invariant, but it also is attractive to $\mathbb{R}_2^+$. Lemma 1 also says that any global stability in Ω is essentially the global stability in $\mathbb{R}_2^+$. We henceforth do our mathematical analysis within the feasible domain Ω.

If we choose $D(x, y) = 1/(xy)$ as a Dulac function, then

$$\frac{\partial(PD)}{\partial x} + \frac{\partial(QD)}{\partial y} = -\nu\mathcal{R}_d\left(\frac{1 - (x + y)}{x^2} + \frac{1}{x} + \frac{1}{y}\right) < 0, (x, y) \in \Omega$$

rules out the possibility of oscillations.

LEMMA 2. *For any parameter values of $\mathcal{R}_0$, $\mathcal{R}_d$, and ν, there is not a closed trajectory to system (2.2).*

Since closed trajectories are impossible, equilibria play a key role in determining the dynamics of the model. We shall analyze it in what follows.
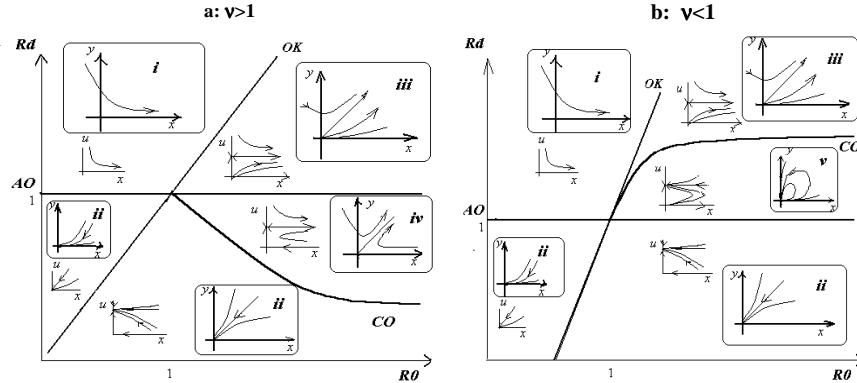
FIGURE 2. *Bifurcation diagram of a positive neighborhood of point O in the $(\mathcal{R}_0, \mathcal{R}_d)$- and (x,y)-planes together with a neighborhood of axis $u = y/x$. **AO** is $\mathcal{R}_d = 1$; **OK** $\mathcal{R}_d = (\nu + \mathcal{R}_0 - 1)/\nu$; and **CO** $\mathcal{R}_d = (\nu - 1 + \mathcal{R}_0)/(\nu\mathcal{R}_0)$. When $\nu > 1$ (see the left figure), region (i) is a saddle sector, (ii) a attracting-node sector, (iii) a saddle and repelling-node sector, and (iv) two saddle sectors. When $\nu < 1$ (see the right figure), regions (i), (ii), and (iii) are the same as that of $\nu > 1$. A new region named (v) represents the elliptic sector.*

3. **Qualitative analysis of simple equilibria.** There are three possible equilibria: $O(0,0)$, $A(1-\mathcal{R}_d^{-1},0)$, and $C(x^*,y^*)$ where $x^* = 1/\mathcal{R}_0 - (\nu + \mathcal{R}_0 - 1)/(\nu\mathcal{R}_0^2\mathcal{R}_d)$ and $y^* = (\mathcal{R}_0 - 1)x^*$.

Equilibrium $O(0,0)$ always exists. However, because neither $P(x,y)$ nor $Q(x,y)$ are *analytic* at this point, the common approach of linearization to discuss the structure and the stability of this equilibrium fails. This issue has not received enough attention in the dynamical analysis of epidemic models, but that is not the case in ecological models (for example, see Arditi and Ginzburg (1989), Kuang and Beretta (1998), Berezovskaya et al. (2001), and Hwang and Kuang (2003)). The structure of the equilibrium point O as a function of the parameters of the system can be seen in Fig. 2. A discussion of how this figure was drawn is provided in section 4.

The second equilibrium $A(1 - \mathcal{R}_d^{-1},0)$ exists inside Ω only if $\mathcal{R}_d > 1$. When sloppy $\mathcal{R}_d = 1$, $A(1 - \mathcal{R}_d^{-1},0)$ coalesces with $O(0,0)$. The local stability of A can be examined by the regular linearization approach, which is determined by the epidemiological basic reproductive number $\mathcal{R}_0$. The Jacobian around A is

$$J_A = \begin{bmatrix} \nu(1 - \mathcal{R}_d) & \nu(2 - \mathcal{R}_d) - \mathcal{R}_0 \\ 0 & \mathcal{R}_0 - 1 \end{bmatrix},$$

hence, $\det(J_A) = \nu(\mathcal{R}_0 - 1)(1 - \mathcal{R}_d)$ and $\mathrm{trace}(J_A) = \mathcal{R}_0 - 1 + \nu(1 - \mathcal{R}_d)$. The analysis of the corresponding linear system leads to proposition 1.

PROPOSITION 1.

1) *If $\mathcal{R}_d > 1$, equilibrium $A(1 - \mathcal{R}_d^{-1},0)$ exists. It is a saddle if $\mathcal{R}_0 > 1$ while it is a stable node when $\mathcal{R}_0 < 1$.*

2) *The phase curves of the system which tends to A are of the form*

$$y = \left(x - (1 - \mathcal{R}_d^{-1})\right)(1 + o(1)) \frac{\mathcal{R}_0 - 1 + \nu(\mathcal{R}_d - 1)}{\nu(2 - \mathcal{R}_d) - \mathcal{R}_0}. \qquad (3.1)$$

If A is a saddle, then formula (3.1) and x-axis (two pieces of positive x-axis cut at A) set its separatrices.

The third potential equilibrium is $C(x^*, y^*)$, where

$$x^* = \frac{1 - 1/(\nu\mathcal{R}_d)}{\mathcal{R}_0} - \frac{1 - 1/\nu}{\mathcal{R}_d\mathcal{R}_0^2} \qquad \text{and} \qquad y^* = (\mathcal{R}_0 - 1)x^*.$$

$C(x^*, y^*)$ exists if

$$\mathcal{R}_d > \frac{(1 - 1/\nu)}{\mathcal{R}_0} + \frac{1}{\nu} \qquad \text{and} \qquad \mathcal{R}_0 > 1 \qquad (3.2)$$

hold. $C(x^*, y^*)$ lies in Ω once it exists because of

$$x^* + y^* = \mathcal{R}_0 x^* = 1 - (\nu\mathcal{R}_0 - 1)/(\nu\mathcal{R}_0\mathcal{R}_d) < 1.$$

When $\mathcal{R}_0 = 1$ and $\mathcal{R}_d > 1$, $C(x^*, y^*)$ coalesces with $A(1 - \mathcal{R}_d^{-1}, 0)$.

The local stability of $C(x^*, y^*)$ can be examined by a routine linearization even though the algebra computations are tedious. The Jacobian of system (2.2) around $C(x^*, y^*)$ is given by

$$J_C = \begin{bmatrix} \frac{\nu + \mathcal{R}_0 - 1}{\mathcal{R}_0} - \nu\mathcal{R}_d\mathcal{R}_0 x^* - \nu - \frac{(\mathcal{R}_0 - 1)^2}{\mathcal{R}_0} & (\nu + \mathcal{R}_0 - 1) - \nu\mathcal{R}_d\mathcal{R}_0 x^* - \frac{1}{\mathcal{R}_0} \\ \frac{(\mathcal{R}_0 - 1)^2}{\mathcal{R}_0} & \frac{1}{\mathcal{R}_0} - 1 \end{bmatrix}.$$

If (3.2) holds, $det(J_C) = \nu(\mathcal{R}_0 - 1)(\mathcal{R}_d\mathcal{R}_0 x^*) > 0$ and $trace(J_C) = -\nu(\mathcal{R}_0 - 1)/\mathcal{R}_0 - (\mathcal{R}_0 - 1)^2/\mathcal{R}_0 - \nu\mathcal{R}_d\mathcal{R}_0 x^* < 0$. Hence, $C(x^*, y^*)$ is always asymptotically stable whenever it exists.

PROPOSITION 2. *If conditions (3.2) holds, equilibrium $C(x^*, y^*)$ exists; and it is an asymptotically stable topological node.*

The global stability of $C(x^*, y^*)$ in $\mathbb{R}_2^+$ can be established by proposition 2, Lemma 1, and Lemma 2.

PROPOSITION 3. *The positive equilibrium $C(x^*, y^*)$ of system (2.2) is globally asymptotically stable in $\mathbb{R}_2^+$ if $(\mathcal{R}_0, \mathcal{R}_d)$ falls in regions 3 and 4 for $\nu > 1$ (Fig. 3) and in region 3 for $\nu < 1$ (Fig. 4).*

4. **Qualitative analysis of the equilibrium point O.** The point O always lies on Ω for any nonnegative parameter values but the vector field is not analytic at O. It is natural to continuously extend the determination of system (2.2) into the origin by changing the independent variable: $\tau \rightarrow (x + y)\tau$. The new system is

$$\frac{dx}{d\tau} = P_1(x, y) \equiv P(x, y)(x + y),$$

$$\frac{dy}{d\tau} = Q_1(x, y) \equiv Q(x, y)(x + y).$$

Because the gradient of $P_1(x, y)$ at $(0, 0)$ vanishes, the isocline $dx/d\tau \equiv \nu\mathcal{R}_d(x + y)^2(1 - (x + y)) - \nu x(x + y) - \mathcal{R}_0 xy = 0$ is a complicated curve in the origin. Hence, the origin is a complicated equilibrium of system (2.2). The structure of trajectories in a small neighborhood of O in Ω depends on parameter values; and it can change in an essential way with a change of parameters. Structure of the point O as well

TABLE 1. Boundaries of phase-parameter portrait.

	equation	property
AO	$\mathcal{R}_d = 1$	appearance/disappearance of **A**
OK	$\mathcal{R}_d = \frac{\nu - 1 + \mathcal{R}_0}{\nu}$ for $\mathcal{R}_0 > 1$	topological structure of **O** changes
CA	$\mathcal{R}_0 = 1$ for $\mathcal{R}_d > 1$	appearance/disappearance of **C**
CO	$\mathcal{R}_d = \frac{\nu - 1 + \mathcal{R}_0}{\nu(\theta(\mathcal{R}_0 + 1) + 1)}$ for $\mathcal{R}_0 > 1$	appearance/disappearance of **C**.

as the asymptotics of trajectories with $(x, y) \to O$ is shown in Figure 2, which is described in Lemma 3.

LEMMA 3. *For different positive values of parameters $\mathcal{R}_0$, ν, and $\mathcal{R}_d$ there exist five types of topologically different structures of the neighborhood of point O in Ω:*

1) *a saddle sector (region (i) in Fig. 2) possessing by separatrix $y = 0$ for parameter values $\mathcal{R}_d > (\nu + \mathcal{R}_0 - 1)/\nu$ and $\mathcal{R}_d > 1$;*
2) *an attracting-node sector region ((ii) in Figure 2) containing a family of trajectories with arbitrary constant $C \neq 0$ that tend to 0 as $t \to \infty$*

$$y = C x^{\frac{\mathcal{R}_0 - 1}{\nu(\mathcal{R}_d - 1)}} (1 + o(1)) \qquad (4.1)$$

for parameter values $1 > \mathcal{R}_d > (\nu + \mathcal{R}_0 - 1)/\nu$;
3) *a saddle sector (region (iii) in Fig. 2) having separatrix*

$$y = \frac{\mathcal{R}_0 - 1 - \nu(\mathcal{R}_d - 1)}{\nu \mathcal{R}_d} x (1 + o(1)) \qquad (4.2)$$

and repelling-node sector containing a family of trajectories given by (4.1) that originate from O (i.e., it tends to O as $t \to -\infty$) if $1 < \mathcal{R}_d < (\nu + \mathcal{R}_0 - 1)/\nu$ and $\nu \geq 1$, or if $1 < (\nu + \mathcal{R}_0 - 1)/(\nu \mathcal{R}_0) < \mathcal{R}_d < (\nu + \mathcal{R}_0 - 1)/\nu$ and $\nu < 1$;
4) *two saddle sectors (region (iv) in Fig. 2a) separated by separatrix given by (4.2) for parameter values $(\nu + \mathcal{R}_0 - 1)/(\nu \mathcal{R}_0) < \mathcal{R}_d < 1$;*
5) *an elliptic sector (region (v) in Fig. 2b) composed by trajectories tending to O as $t \to \infty$ (with asymptotics given by (4.2)) as well as with $t \to -\infty$ (family given by (4.1)) if $1 < \mathcal{R}_d < (\mathcal{R}_0 - 1 + \nu)/(\nu \mathcal{R}_0)$.*

An elliptic sector is defined as a family of homoclinics that contains no any equilibrium. Using the version of the blow-up method associated with the Newton diagram (Berezovskaya (1976, 1995)), Lemma 3 is proved in Appendix A.

5. **Phase-parameter portraits.** In this section we focus on the (x, y)- and $(\mathcal{R}_0, \mathcal{R}_d, \nu)$-parameter portrait to system (2.2) that is obtained from the cuts on the $(\mathcal{R}_0, \mathcal{R}_d)$-plane generated by fixed values of ν. Four curves, **AO**, **CA**, **CO**, and **OK**, partition the parameter space. Their equations are listed in Table 1. The cut of the parameter portrait on the $(\mathcal{R}_0, \mathcal{R}_d)$-plane essentially depends on the value ν. The phase-parameter portraits in (x, y) and $(\mathcal{R}_0, \mathcal{R}_d)$-planes for the two cases of $\nu > 1$ and $\nu < 1$ are given in Figures 3 and 4. Curve **AO** corresponds to the appearance or disappearance of equilibrium A. Equilibrium $C(x^*, y^*)$ coalesces with $A(1 - \mathcal{R}_d^{-1}, 0)$ on $\mathcal{R}_0 = 1$ and $\mathcal{R}_d > 1$ (on the curve **CA**). The values $\mathcal{R}_d = (\nu + \mathcal{R}_0 - 1)/(\nu \mathcal{R}_0)$ (on curve **CO**) correspond to the coalescing of point C and O.

TABLE 2. Parameter values in phase portraits of Figure 5.

	1a	1b	2	3a	3b	4
$\mathcal{R}_0$	0.9	1.5	0.9	1.5	1.1	2.0
$\mathcal{R}_d$	0.9	0.5	1.2	1.3	1.2	0.9

TABLE 3. Parameter values in phase portraits of Figure 6.

	1a	1b	2	3a	3b	4
$\mathcal{R}_0$	0.3	1.8	0.9	0.7	1.1	2.0
$\mathcal{R}_d$	0.5	0.8	3.0	3.0	3.0	3.0

The main result of our investigation is collected in Theorem 1.

THEOREM 1. *The space of nonnegative parameters $(\mathcal{R}_0, \mathcal{R}_d, \nu)$ for system (2.2) is subdivided into five domains of topologically different phase portraits belonging to Ω. The cuts of parameter space corresponding to fixed values of ν are given in Figure 3 for $\nu > 1$ and Figure 4 for $\nu < 1$. The boundary surfaces between domains correspond to the following bifurcations for system (2.2):*

AO *distinguishes the appearance or disappearance of the equilibrium point A;*

OK *specifies the change of topological structure of the equilibrium point O;*

CO *and* **CA** *give rise to the appearance or disappearance of the equilibrium point C.*

If $\mathcal{R}_0 = \mathcal{R}_d = 1$, system (2.2) is integrable and trajectories are of the form

$$(x + y)^2 - y^2 \frac{2\nu - 1}{2\nu y + cy^{2\nu}} = 0,$$

where c is an arbitrary constant.

If $\nu = 1$, the equation for N has a close form $dN/dt = \mathcal{R}_d N(1 - N) - N$, and $\mathcal{R}_d = 1$ is the only critical value. If $\mathcal{R}_d < 1$, $O(N = 0)$ is asymptotically stable; if $\mathcal{R}_d > 1$ then $A(N = 1 - \mathcal{R}_d^{-1})$ is asymptotically stable. Formally, curves **CO** and **AO** are identical for $\nu = 1$. The phase-parameter portrait consists only of regions 1, 2, and 3 (see Figures 3 and 4). Hence, if $\mathcal{R}_d > 1$ the total population size tends to $1 - \mathcal{R}_d^{-1}$, otherwise the population goes to extinction.

All boundary surfaces correspond to bifurcations of co-dimension one (the total number of "connections" between parameters) in system (2.2). The lines of intersection or touching between the boundary surfaces correspond to bifurcations of co-dimension two (see Kuznetsov (1995)). Figures 3 and 4 represent correspondingly the three-dimensional parameter portrait of the system as a cross-section into the $(\mathcal{R}_0, \mathcal{R}_d)$-plane for $\nu > 1$ and $\nu < 1$.

Our theoretical analysis is confirmed by the numerical simulations. Some typical phase portraits of the system can be seen from Figures 5 and 6. The parameter values in these simulations are listed in Tables 2 and 3. We are particularly interested in the occurrence of a family of homoclinic trajectories (see Figure 8), which occurs when the parameters are in domain 5 in Figures 4 and 7.

6. **Exploration of parameter θ.** The incorporation of parameter θ into model (1.1) demographically marks susceptibles and infectives, the two epidemiological units, in terms of their reproductive capability to the total population. Infected individuals may reduce their reproduction because of, the illness or their offsprings

may be quarantined (or removed) immediately from the population, thus decreasing the recruitment rate into the population. If the disease has no impact on the reproductive process, then $\theta = 1$; if the disease leads to a complete loss of reproductivity

TABLE 4. Global attractor of system (1.1).

parameter	globally asymptotic attractor
$\mathcal{R}_0 < 1$, $\mathcal{R}_d < 1$	$(0,0)$
$\mathcal{R}_0 < 1 < \mathcal{R}_d$	$(1 - \mathcal{R}_d^{-1}, 0)$
$1 < \mathcal{R}_0$, $\frac{\nu + \mathcal{R}_0 - 1}{\nu(\theta(\mathcal{R}_0 + 1) + 1)} < \mathcal{R}_d$	(x_θ^*, y_θ^*)
$1 < \mathcal{R}_0$, $1 < \mathcal{R}_d < \frac{\nu + \mathcal{R}_0 - 1}{\nu(\theta(\mathcal{R}_0 + 1) + 1)}$, $\nu\theta < 1$	$(0,0)$ (elliptic sector appears)
$\mathcal{R}_d < 1$, $1 < \mathcal{R}_0$, $\nu\theta < 1$	$(0,0)$
$1 < \mathcal{R}_0$, $\mathcal{R}_d < \frac{\nu + \mathcal{R}_0 - 1}{\nu(\theta(\mathcal{R}_0 + 1) + 1)}$, $\nu\theta > 1$	$(0,0)$

of the infected individuals, or if new births born to them cease, are removed, $\theta = 0$. These two extreme situations are more important since it is hard to find a partial loss of reproductivity or partial cessation of new births.

We have systematically studied the special case of $\theta = 1$ in previous sections. Although model (2.1) is a sub-model of (1.1), our results are general. Model (1.1) is written in the form

$$\begin{cases} \frac{dx}{d\tau} = \nu\mathcal{R}_d(x + \theta y)(1 - (x + y)) - \nu x - \mathcal{R}_0 \frac{xy}{x+y} \equiv P_\theta(x, y) \\ \frac{dy}{d\tau} = -y + \mathcal{R}_0 \frac{xy}{x+y} \equiv Q_\theta(x, y). \end{cases} \quad (6.1)$$

Technically, all arguments about model (2.1) can be applied to model (1.1). We briefly list the results here. Lemmas can be applied to model (6.1) no change. The infection-free equilibrium of system (6.1) $A(1 - \mathcal{R}_d^{-1}, 0)$ exists if $\mathcal{R}_d > 1$; and the endemic equilibrium $C(x_\theta^*, y_\theta^*)$ with

$$x_\theta^* = (\nu\mathcal{R}_d(\theta(\mathcal{R}_0 - 1) + 1) - (\nu + \mathcal{R}_0 - 1))/(\nu\mathcal{R}_0\mathcal{R}_d(\theta(\mathcal{R}_0 - 1) + 1)), \quad (6.2)$$

$$y_\theta^* = (\mathcal{R}_0 - 1)x_\theta^* \quad (6.3)$$

exists if $\mathcal{R}_0 > 1$ and $\mathcal{R}_d > (\nu + \mathcal{R}_0 - 1)/((\theta\nu(\mathcal{R}_0 - 1) + 1))$. Similar to Lemma 3, the phase-parameter portrait for system (1.1) is described in Lemma 4.

LEMMA 4. *For positive values of parameters $\mathcal{R}_0$, ν, $\mathcal{R}_d$, and $0 < \theta \leq 1$ there exist five types of topologically different structures of the positive neighborhood of point O described by Lemma 3 and shown in Figure 2. The boundaries AO and OK are the same as in Lemma 3 and CO is $\mathcal{R}_d = (\nu + \mathcal{R}_0 - 1))/(\nu(\theta(\mathcal{R}_0 - 1) + 1))$ (see Table 1). Accordingly Figure 2 shows the bifurcation diagram of O for $\nu\theta > 1$ and for $\nu\theta < 1$.*

Basing on Lemma 4 we can formulate Theorem 2 to system (6.1).

THEOREM 2. *The bifurcation diagram of system (6.1) with $0 < \theta \leq 1$ is given in Figure 3 for $\nu\theta > 1$, in Figure 4 for $\nu\theta < 1$, and additionally in Figure 7 for $\theta = 0$.*

Figure 7 gives a full description to the global dynamics of model (1.1) in the case of $\theta = 0$. Comparing Figure 7 with Figures 3 and 4, we can see that region 4 disappears, region 3 narrows, and, consequently, region 1 where the population
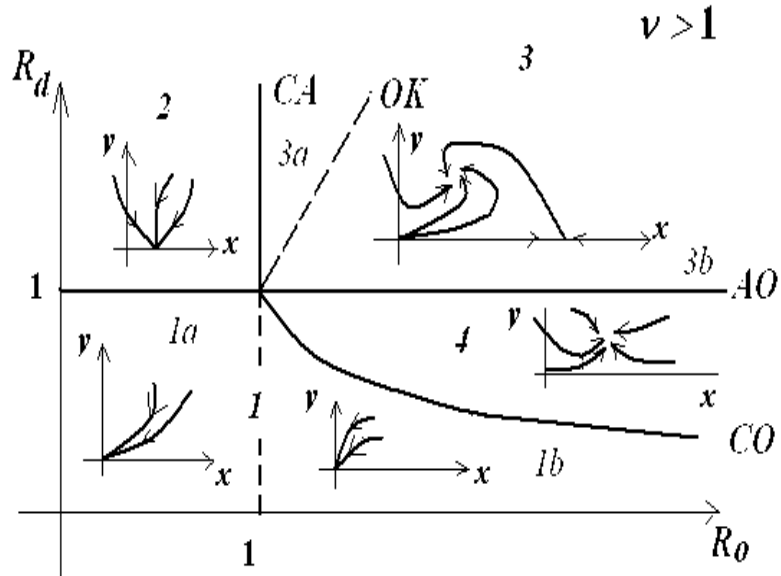
FIGURE 3. *Phase-parameter portraits of model (2.2) given as an $(\mathcal{R}_0, \mathcal{R}_d)$-cut of the positive parameter space $(\mathcal{R}_0, \mathcal{R}_d, \nu)$ for arbitrary fixed changes in behavior, and their equations are listed in Table 1.*
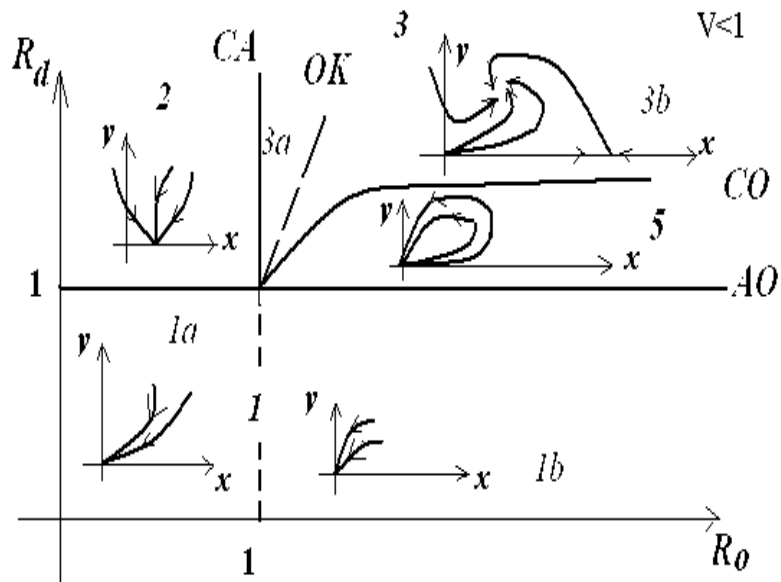
FIGURE 4. *Phase-parameter portraits of model (2.2) given as an $(\mathcal{R}_0, \mathcal{R}_d)$-cut of the positive parameter space $(\mathcal{R}_0, \mathcal{R}_d, \nu)$ for arbitrary fixed value of $\nu < 1$. The boundaries are the same as in Fig. 3.*

goes to extinction, dramatically expands. This demonstrates that the reduction of reproductivity of infected individuals will increase the likelihood of extinction of the entire population. A full picture of the global dynamics of model (1.1) can be found in Table 4.

7. **Discussion and conclusions.** A *simple* epidemic model is completely studied. The selection and relevance of the model is not the key issue (albeit we will use it to interpret our results) but rather the approach to the study of its dynamics near O, the equilibrium where both the population and the disease die out (note that this equilibrium is observed in populations where N grows exponentially; the population here, however, is bounded). Hence, the *main* purpose is to highlight the nature and richness of the dynamics near regions where the vector field is *not* analytic, a *common* situation in epidemiological modeling that has not been analyzed well.

Mathematically the qualitative behaviors supported by model (1.1) in response to the changes of four dimensionless parameters $\mathcal{R}_0$, $\mathcal{R}_d$, θ, and ν are well understood from our investigation; that is, we study the qualitative nature of the dynamics as a function of epidemiological, demographic, and "relative" removal parameters. As can be seen from Table 4, there are three qualitatively different dynamics for all possible parameter values.

1) Extinction of the population is realized for values in domain 1 (Fig. 3) and in domains 1 and 5 (Fig. 4). This is observed for any initial ratio of the susceptible and infectious subpopulations, since the $O(0,0)$ is a global attractor;

2) The disease dies out and the population recovers if the parameters are in domain 2 of Figures 3 and 4; that is, the number of infectious vanishes as t grows;

3) The invasion of the disease into the populations is successful if the parameters are in domains 3 and 4 for $\nu > 1$ (Fig. 3) and in domain 3 for $\nu < 1$ (Fig. 4).

Comparing these results with those obtained for model (2.1) under a constant population size (see Fig. 1) leads one to conclude that the dynamics of system (2.2) near the equilibrium $O(0,0)$ is responsible for the "novel" dynamics. This novel behavior takes place in the domains of extinction in Figures 3 and 4; that is, in the regions where the origin is the only attractor.

Two additional important dynamics demonstrate "paradoxical" behaviors from the model, which happens if the parameters fall in region 4 of Figure 3 and region 5 of Fig. 4.

Paradox one is that the total population survives, although the basic demographic reproductive number $\mathcal{R}_d$ is less than one. This is observed conditionally because we have to assume additionally $\nu = (\mu + m)/(\mu + d) > 1$ and $\mathcal{R}_d > (1 + (\nu - 1)/\mathcal{R}_0)/\nu$. The migration of susceptibles plays a key role in making $\nu = (\mu + m)/(\mu + d) > 1$. It is noted that $\nu = (\mu + m)/(\mu + d) > 1$ is equivalent to $m > d$, meaning that the per-capita migration rate of susceptible populations surpasses the death rate due to the disease. However, the basic demographic reproductive number $\mathcal{R}_d$ cannot be too small. The lower bound for $\mathcal{R}_d$ to support this paradox is $(1 + (\nu - 1)/\mathcal{R}_0)/\nu$.

The second paradox is that the total population goes extinct even for recruitment of susceptibles $\mathcal{R}_d > 1$. Again this is conditional because we need additionally to assume $\nu < 1$, $1 < \mathcal{R}_0$, and $\mathcal{R}_d < (1 - (1-\nu)/\mathcal{R}_0)/\nu$; that is, the migration rate m is
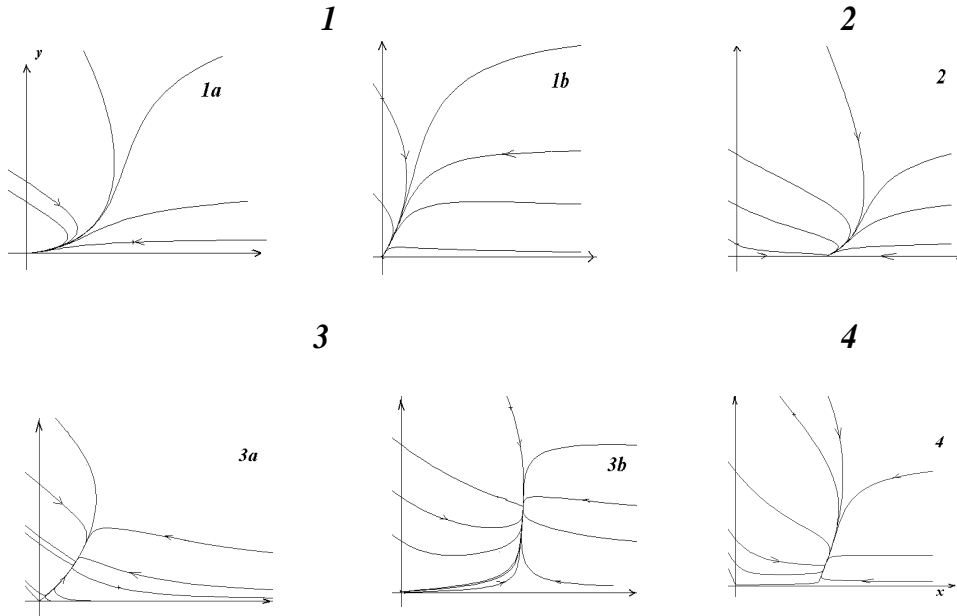
FIGURE 5. *Phase portraits of the model for $\nu = 1.8 > 1$, (numeration of domain corresponds to those in Fig. 3). Values of $\mathcal{R}_0$ and $\mathcal{R}_d$ are given in table 2.*
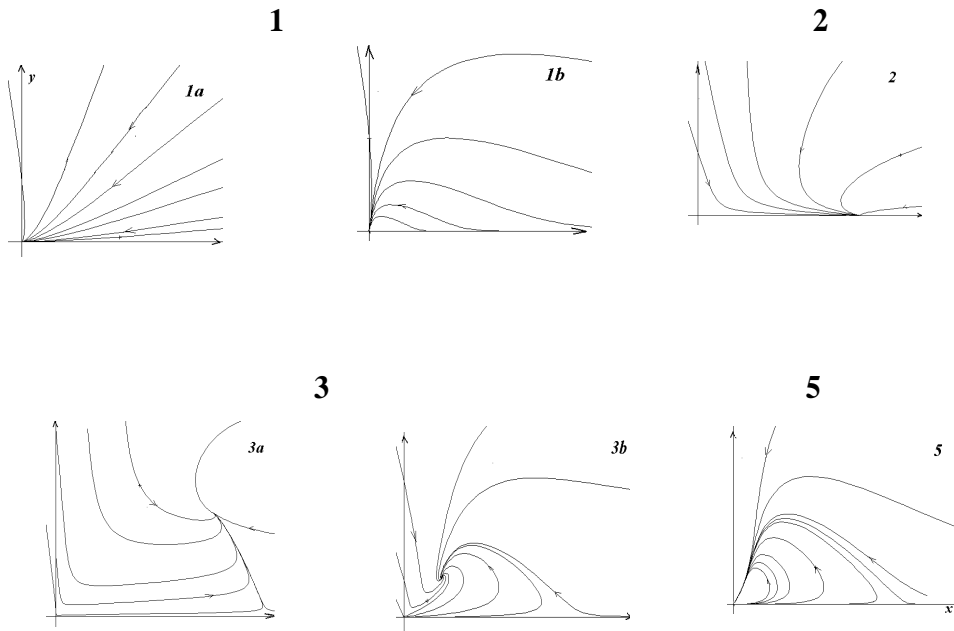

FIGURE 6. *Phase portraits of the model for $\nu = 0.2 < 1$ (numeration of domain corresponds to those in Fig. 4). Values of $\mathcal{R}_0$ and $\mathcal{R}_d$ are given in table 3*

less then the disease-induced death rate d, but the basic demographic reproductive number $\mathcal{R}_d$ must be bounded from above. The upper bound is $(1 - (1 - \nu)/\mathcal{R}_0)/\nu$.

The appearance of *an elliptic attractor* highlights the possibility of a *disease outbreak*, even though the population is becoming extinct. The reason behind this behavior is that the demographic and epidemiological processes support different growth rates at the "beginning" of the epidemic. The fact that the epidemiological process is faster than the demographic process leads to an increase in the number of infections, even though the total (bounded) population will go eventually extinct. This behavior, to the best of our knowledge, has never been reported in the context of epidemiological models.

The role of parameter θ is included in theorem 2, which allows us to reveal the implication of the fecundity of infectives and migrations. The threshold $\nu = 1$ of system (2.2) is replaced by the threshold $\theta\nu = 1$ for model (1.1). More specifically, if $\theta\nu > 1$, then the disease dies out and population recovers in region 2 ($\mathcal{R}_0 < 1$); and the disease successfully invades the population if the parameters are in regions 3 and 4 ($\mathcal{R}_0 > 1$) of Figure 3. If $\theta\nu < 1$, the whole population persists only if the parameters are in domains 2 and 3 in Figure 4. The decreasing of θ leads to the decreasing of domain 3 and in creasing of domain 5 (see Figures 4 and 7). Consequently, the chance of a disease outbreak increases. The phase-parameter portraits of models (2.2) and (6.1) are equivalent, so the principal qualitative behaviors of these two models are the same.

If $\nu\theta \leq 1$ then the total population goes extinct, even if the demographic parameter $\mathcal{R}_d > 1$ but with $\nu\mathcal{R}_d \leq (\nu + \mathcal{R}_0 - 1)/(\theta(\mathcal{R}_0 - 1) + 1)$ and $\mathcal{R}_0 > 1$. In this parameter region the growth of susceptibles is observed for small initial values of infectives. Both susceptibles and infectives increase initially, if the infected part of the population is relatively small; then most of the population becomes infected and the total population goes extinct. This plausible behavior of the model corresponds to a family of homoclinics at the origin and is the same as in the case $\theta = 1$. Our analytical investigation has proved that the elliptic sector is realized for model (1.1) with parameter values belonging to domain 5.

The case $\nu\theta > 1$ realizes only if $\nu > 1$ (that is, if the migration rate of is relatively large). Paradoxically, in this case infectives and susceptibles can persist even for demographic parameter $\mathcal{R}_d < 1$ if we additionally assume $\nu\mathcal{R}_d \geq (\nu + \mathcal{R}_0 - 1)/(\theta(\mathcal{R}_0 - 1) + 1)$ and $\mathcal{R}_0 > 1$.

An important ecological (and evolutionary) problem is to determine the necessary and sufficient conditions under which a disease can regulate a population (see, for example, Levin and Pimentel (1981), Anderson et al. (1988, 1989) and Song et al. (2002)). The work on this question has not used models that include migration. Our model can be thought of as an example of a system where individuals avoid the disease by migrating to a disease-free habitat. The inclusion of disease-induced mortality and migration can lead to the novel dynamics near the origin O.

It is our hope that the analysis of this example may influence the field of theoretical epidemiology, as has already occurred in the field of ecology, where these model results have been used to explain the "paradox of biological control" (see Arditi and Ginzburg (1989), Kuang and Beretta (1998), Berezovskaya et al. (2001), and Hsu et al. (2001)).

Typically, two forms of incidence rates βSI and $\beta SI/N$ are used to model most epidemic processes. βSI (known as the *mass action law*) assumes that transmission depends linearly on population size, while $\beta SI/N$ assumes that infectives are
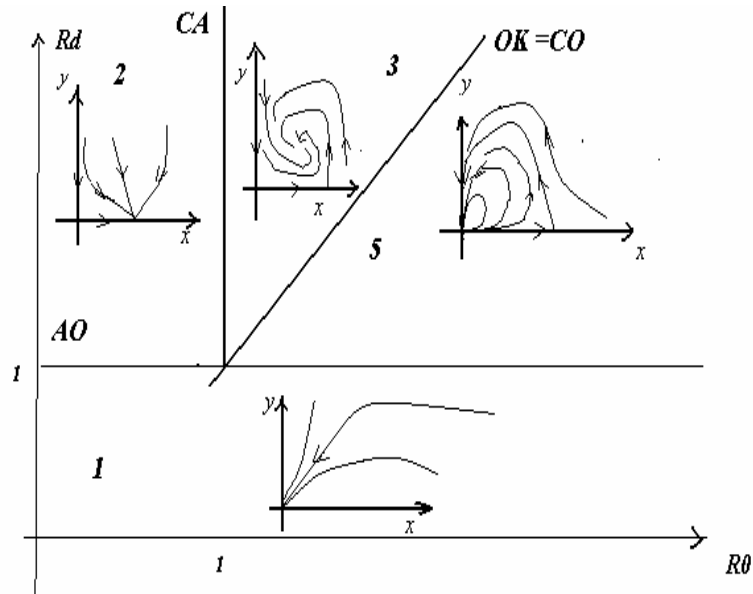
FIGURE 7. *The phase-parameter portrait of model (6.1) for $\theta = 0$ given as an $(\mathcal{R}_0, \mathcal{R}_d)$-cut of the positive parameter space $(\mathcal{R}_0, \mathcal{R}_d, \nu)$ for an arbitrary fixed value of ν. The boundaries have the same sense as in Figures 3 and 4; and they are defined in Table 1.*
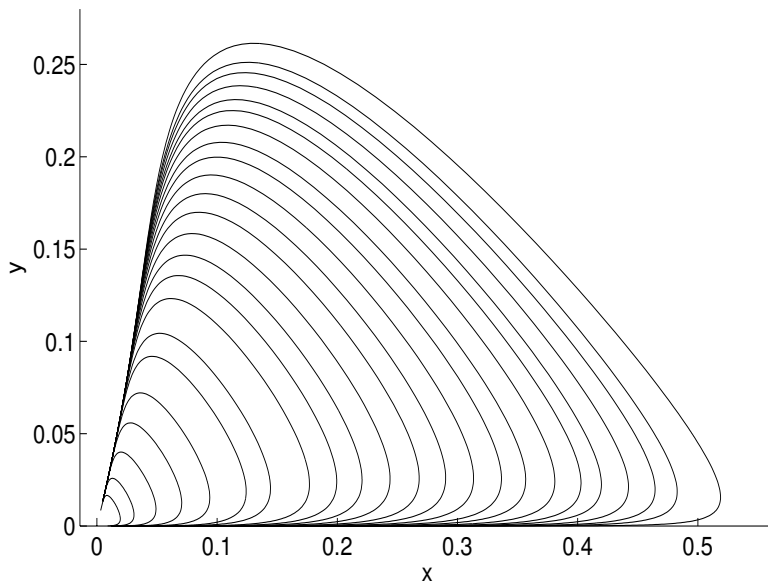

FIGURE 8. Homoclinic trajectories.

contacted at random (transmission is independent of N). The dynamics obtained in model (2.2), where random mixing is assumed, are not supported under the *mass action law* $\beta S I$. Other researchers have used $\beta S^\alpha I^\gamma$ (Liu et al. (1987,1986)) to model the incidence rate for a variety of reasons. The novel dynamics of this paper cannot be obtained with these forms of the incidence rate either. Ruan and Wang (2003) have recently introduced $\beta S I^l / (1 + \alpha I^h)$ to model the incidence rate in a model without disease-induced death rate (an analytic vector field is generated in this case). The dynamics in the model using this incidence rate have been characterized by saddle-node, Hopf, homoclinic bifurcations, and possible multiple limit cycles. However, although the dynamics are rich and interesting, we have found no reasonable way of explaining an appropriate epidemiological setting for this nonlinearity.

Appendix A. **Proof of Lemmas 3 and 4.**

Proof. The proof of Lemma 4 is given first. System (6.1) (and its particular case (2.2)) is analytical in all points of the plane (x, y) except the origin. The positioning of its phase trajectories in the first quadrant can be defined from the following polynomial system:

$$\begin{cases} \frac{dx}{d\tau} = \nu \mathcal{R}_d(x + \theta y)(1 - (x + y))(x + y) - \nu x(x + y) - \mathcal{R}_0 xy \equiv P_1(x, y), \\ \frac{dy}{d\tau} = -y(x + y) + \mathcal{R}_0 xy = (\mathcal{R}_0 - 1)xy - y^2 \equiv Q_1(x, y) \end{cases} \quad \text{(A.1)}$$

System (A.1) is transferred from (6.1) by rescaling $x = cX$, $y = cY$, and $dt = (x + y)/(\mu + d)d\tau$. System (A.1) has a complicated equilibrium point at the origin because both eigenvalues are equal to zero. We then perform a blow-up transformation plus a rescaling to system (A.1) by

$$x = x, \qquad u = y/x, \quad \text{(A.2)}$$
$$x d\tau = ds \quad \text{(A.3)}$$

This transforms $\mathbb{R}_+^2$ of the (x, y)-plane in a nondegenerate way, except for $x = 0$ into $\mathbb{R}_+^2$ of the (x, u)-plane and blows up the point O into the u-axis. Structurally, the transformation $y = ux$ leaves the pattern on the $x > 0$ half (x, u)-plane "qualitatively unchange." On the $x < 0$ half plane, the pattern is reflected across the $x-$axis and then the entire $u-$axis is collapsed into one point. This transformation intends to break a complex equilibrium into several simple equilibria. Under the transformations (A.2) and (A.3), we obtain the system

$$\begin{cases} \frac{dx}{ds} = x(\nu \mathcal{R}_d \theta u^2 + (\nu \mathcal{R}_d(1 + \theta) - \nu - \mathcal{R}_0)u \\ \qquad + \nu(\mathcal{R}_d - 1)) - \nu \mathcal{R}_d x^2 (1 + \theta u)(1 + u)^2 \\ \frac{du}{ds} = -u(1 + u)(\nu \mathcal{R}_d \theta u - Z) + \nu \mathcal{R}_d x u(1 + \theta u)(1 + u)^2, \end{cases} \quad \text{(A.4)}$$

where

$$Z = \mathcal{R}_0 - 1 - \nu(\mathcal{R}_d - 1). \quad \text{(A.5)}$$

TABLE 5. Eigenvalues of (A.4) around O_1 and K_1

equilibrium	λ_1	λ_2
O_1	$\nu(\mathcal{R}_d - 1)$	Z
K_1	$\dfrac{(\nu\mathcal{R}_d - 1)\mathcal{R}_0 - (\nu-1)}{\nu\mathcal{R}_d}$	$-\dfrac{Z(Z + \nu\mathcal{R}_d)}{\nu\mathcal{R}_d}$

System (A.4) has two feasible equilibria on the u-axis: $O_1(0,0)$ and $K_1(0, Z/(\nu\mathcal{R}_d\theta))$. The eigenvalues of the Jacobian matrix at these equilibria are listed in Table 5. So, these equilibrium points are nondegenerate if

$$(\nu\mathcal{R}_d\theta(\mathcal{R}_0 - 1) - Z)Z(\mathcal{R}_d - 1) \neq 0.$$

The equilibria are classified into six qualitatively different combinations.

1) single saddle O_1 if $\mathcal{R}_d > 1$ and $Z < 0$ ($\mathcal{R}_d > (\mathcal{R}_0 - 1)/\nu + 1$);
2) single stable node O_1 if $\mathcal{R}_d < 1$ and $Z < 0$. These inequalities imply system $(\mathcal{R}_0 - 1)/\nu + 1 < \mathcal{R}_d < 1$, which has solutions only if $\mathcal{R}_0 < 1$;
3) saddle O_1 and stable node K_1 if $Z > 0$, $\mathcal{R}_d < 1$, and $(-Z + \nu\mathcal{R}_d\theta(\mathcal{R}_0 - 1)) < 0$. These inequalities imply system: $\mathcal{R}_d < 1$, $\mathcal{R}_d < 1 + (\mathcal{R}_0 - 1)/\nu$, and $\nu\mathcal{R}_d < (\nu + \mathcal{R}_0 - 1)/(\theta(\mathcal{R}_0 - 1) + 1)$, which has solutions $\mathcal{R}_0 > 1$, $\nu\theta > 1$ as well as $\mathcal{R}_0 < 1$, $\nu\theta < 1$;
4) saddle O_1 and saddle K_1 if $Z > 0$, $\mathcal{R}_d < 1$, and $(-Z + \nu\mathcal{R}_d\theta(\mathcal{R}_0 - 1)) > 0$ that hold true for $(\mathcal{R}_0 - 1 + \nu)/(\nu(1 + \theta\mathcal{R}_0 - 1)) < \mathcal{R}_d < 1$ and implies $\nu\theta > 1$ for $\mathcal{R}_0 > 1$;
5) unstable node O_1 and saddle K_1 if $Z > 0$, $\mathcal{R}_d > 1$, and $(-Z + \nu\mathcal{R}_d\theta(\mathcal{R}_0 - 1)) > 0$. These inequalities hold for $\mathcal{R}_0 > 1$, $(\nu + \mathcal{R}_0 - 1)/(\nu(\theta(\mathcal{R}_0 - 1) + 1)) < \mathcal{R}_d < 1 + (\mathcal{R}_0 - 1)/\nu$;
6) unstable node O_1 and stable node K_1 if $Z > 0$, $\mathcal{R}_d > 1$, and $(-Z + \nu\mathcal{R}_d\theta(\mathcal{R}_0 - 1)) < 0$ hold true for $1 < \mathcal{R}_d < (\mathcal{R}_0 - 1 + \nu)/(\nu(1 + \theta(\mathcal{R}_0 - 1)))$ and implies $\nu\theta < 1$ for $\mathcal{R}_0 > 1$.

To study the behavior of the system close to the y-axis, we should do a blow-up transformation again by $y = y$ and $w = x/y$ with rescaling $yd\tau = ds$. This transformation is nondegenerate for all values of x and y except for $y = 0$, and the point O blows up into the w-axes under this transformation. In terms of variables w and y, we obtain the following system:

$$\begin{cases} \frac{dw}{ds} = (w+1)(-Zw + \nu\mathcal{R}_d\theta) - \nu\mathcal{R}_d y(w+1)^2(w+\theta), \\ \frac{dy}{ds} = y(-1 + (\mathcal{R}_0 - 1)w), \end{cases} \quad \text{(A.6)}$$

which has, on the w-axis, a feasible equilibrium $K_2^*(k_2^*, 0)$ with $k_2^* = \nu\mathcal{R}_d\theta/Z$. It turns out that it is not necessary to study points K_2^*, because it corresponds to the equilibrium K_2 of system (A.4). If $\theta = 0$, then $O_2(0,0)$ is a "new" equilibrium that is a saddle if $Z < 0$, and a stable node if $Z > 0$.

Behaviors of system (1.1) for $\theta = 1$ in a positive neighborhood of axis u, and behaviors of system (A.1) in a positive neighborhood of the complicated equilibrium point $\mathbf{O}$ in the (x,y)-plane dependently on parameters $\mathcal{R}_0$ and $\mathcal{R}_d$ are shown in Figure 2a for $\nu > 1$ and Figure 2b for $\nu < 1$.

It is easy to see from the eigenvalues that for $\nu\theta > 1$ the bifurcation diagram of point O is the same as the diagram for $\nu > 1$ and $\theta = 1$, as shown in Figure 2a,

and for $\nu\theta < 1$ it is the same as the diagram for $\nu < 1$ and $\theta = 1$, as shown in Figure 2b.

The analysis of the case $\theta = 0$ demands the mutual consideration of the positive neighborhoods of axes for u and w. There are three possible type of structures: (1) a saddle sector whose separatrices are $u = 0$ for $v > 0$ and $v = 0$ for $u > 0$ if the parameters are $Z < 0$ and $\mathcal{R}_d > 1$ (like (i) in Fig. 2); (2) a stable parabolic sector if parameters $Z < 0$ and $\mathcal{R}_d < 1$ (like (ii) in Fig. 2a); and (3) an elliptic sector belonging to the positive quadrant (u, v) for $Z > 0$, $\mathcal{R}_d > 1$, and $-Z + \nu\mathcal{R}_d\theta(\mathcal{R}_0 - 1) < 0$ implying $\nu\theta < 1$ for $\mathcal{R}_0 > 1$ (like (v) in Fig. 2b).

Assembling the obtained results and returning to the initial variables x and y, we obtain six different structures of the complicated point O in the first quadrant of (x, y)-plane as shown in Figure 2. Two typical phase portraits of point O (the cases (ii) presented in Figures 3 and 4) are topologically equivalent and differ only in the asymptotes of characteristic trajectories. They should be pooled together in the "unified" phase portrait. Therefore, there are only five topologically different structures in a neighborhood of the equilibrium point **O** for nondegenerate cases.

This ends the proof of Lemma 4.

The above analysis also presents a possibility to show the asymptotics of trajectories that tend to the equilibrium O (here we will consider only the case $\theta = 1$).

Equilibrium $K_1(0, Z/(\nu\mathcal{R}_d))$ of system (A.4) is inside the first quadrant if $Z > 0$. It can be a saddle or a stable node. If K_1 is a saddle (in the case $(\nu\mathcal{R}_d - 1)\mathcal{R}_0 - (\nu - 1) < 0$), then the curve $u = Z/(\nu\mathcal{R}_d)(1 + o(1))$ is the asymptotics of the separatrix. Therefore, the curve

$$y = \frac{Z(1 + o(1))}{\nu\mathcal{R}_d}x \tag{A.7}$$

is a separatrix of the saddle sector of point O. If K_1 is a node, then (A.7) shows that asymptotics of trajectories tend to O.

Equilibrium O_1 of system (A.4) can be a saddle or a node. If it is a node (it happens if $Z(\mathcal{R}_d - 1) > 0$), then in the (x, u)-plane the family of trajectories having the form of $u = Cx^{(\mathcal{R}_0 - 1)/(\nu(\mathcal{R}_d - 1) - 1) + 1}(1 + o(1))$ is tending to it (where C is an arbitrary constant). In terms of x and y, this family is $y = Cx^{(\mathcal{R}_0 - 1)/(\nu(\mathcal{R}_d - 1))}(1 + o(1))$ which tends to $(0, 0)$ as $x \to 0$ (see Fig. 2). This completes the investigation of point O in cases of nondegeneracy.

Finally, if $\mathcal{R}_d = 1$ and $\mathcal{R}_0 = 1$, then $Z = 0$ and, consequently, system (A.6) is reduced to

$$\frac{dw}{dy} = -\nu\left(\frac{w+1}{y} - (w+1)^3\right),$$

which can be solved explicitly, as follows

$$w + 1 = \pm\sqrt{\frac{2\nu - 1}{c - \nu y^{-2\nu+1}}},$$

where c is an arbitrary constant. Proof of Lemma 3 is complete. $\qquad\square$

REFERENCES

[1] R. M. Anderson and R. M. May, *Infectious Diseases of Humans: Dynamics and Control*, Oxford University Press, New York, 1991.

[2] R. M. Anderson, R. M. May and A. R. Mclean, Possible demographic impact of AIDS in developing countries, *Nature* **332** (1988) 228–234.

[3] J. P. Aparacio, A. F. Capurro and C. Castillo-Chavez, Transmission and dynamics of tuberculosis on generalized households, *J. Theor. Biol.* **206** (2000) 327–341.

[4] R. Arditi and L. R. Ginzburg, Coupling in predator-prey dynamics: ratio-dependence, *J. Theor. Biol.* **139** (1989) 311–326.

[5] F. S. Berezovskaya, About asymptotics of trajectories of a system of two differential equations, Report deposited in the All-Union Information Center (USSR), No 3447-76, 17 p. (in Russian), 1976.

[6] F. S. Berezovskaya, The main topological part of plane vector fields with fixed Newton diagram, in *Proceedings on Singularity Theory*, D.T. Le, K. Saito and B. Teissier (eds.), 55-73, Word Scientific, Singapore, New Jersey, London, Hong Kong, 1995.

[7] F. S. Berezovskaya, G. Karev and R. Arditi, Parametric analysis of the ratio-dependent predator-prey model, *J. Math. Biol.* **43**(3) (2001) 221–246.

[8] F. Brauer and C. Castillo-Chavez, *Mathematical Models in Population Biology and Epidemiology*, Springer-Verlag, New York, 2001.

[9] S. Busenberg and K. L. Cooke, *Vertically Transmitted Diseases: Models and Dynamics*, Springer-Verlag, New York, 1983.

[10] C. Castillo-Chavez with S. Blower, P. van den Driessche, D. Kirschner, and A.-A. Yakubu (eds.), *Mathematical Approaches for Emerging and Reemerging Infectious Diseases: An Introduction, IMA, Vol. 125*, Springer-Verlag, New York, 2002.

[11] C. Castillo-Chavez with S. Blower, P. van den Driessche, D. Kirschner, and A.-A. Yakubu (eds.), *Mathematical Approaches for Emerging and Reemerging Infectious Diseases: Models, Methods and Theory, IMA, Vol. 126*, Springer-Verlag, New York, 2002.

[12] C. Castillo-Chavez, *Mathematical and Statistical Approaches to AIDS Epidemiology*, Lecture Notes in Biomathematics 83, Springer-Verlag, Berlin, Heidelberg, 1989.

[13] C. Castillo-Chavez, Mathematical Models for the Spread of HIV/AIDS (Mtg. Review), *Mathematical Biology Newsletter* **3**(1) (1988). 4–5.

[14] O. Diekmann and J. A. P. Heesterbeek, *Mathematical Epidemiology of Infectious Diseases*, Wiley, New York, 2000.

[15] Z. Feng, C. Castillo-Chavez and A. F. Capurro, A model for tuberculosis with exogenous reinfection, *Theoretical Population Biology* **57** (2000) 235–247.

[16] K. P. Hadeler and C. Castillo-Chavez, A core group model for disease transmission, *J. Math. Biosci.* **128** (1995) 41–55.

[17] K. R. Heiderich, W. Huang and C. Castillo-Chavez, Nonlocal response in simple epidemiological model, in *Mathematical Approaches for Emerging and Reemerging Infectious Diseases: Models, Methods and Theory*, C. Castillo-Chavez with S. M. Blower, P. van den Driessche, D. Kirschner, and A.-A. Yakubu (eds.), Springer-Verlag, New York, 2002.

[18] H. W. Hethcote, The mathematics of infectious diseases, *SIAM, Review* **42**(4) (1999) 599–653.

[19] H. W. Hethcote and J. A. Yorke, *Gonorrhea transmission and control, Lectures Notes in Biomathematics* **56** (1984) 1–105.

[20] S.-B Hsu, T.-W. Hwang and Y. Kuang, Global analysis of the Michaelis-Menten type ratio-dependent predator-prey system, *J. Math. Biol.* **432** (2001) 489–506.

[21] T.-W. Hwang and Y. Kuang, Deterministic extinction effect of parasites on host populations, *J. Math. Biol.* **46** (2003) 17–30.

[22] W. O. Kermack and A. G. McKendrick, A contribution to the mathematical theory of epidemics, *Proc. R. Soc.* London, Ser. **A115** (1927) 700–721.

[23] W. O. Kermack and A. G. McKendrick, A contribution to the mathematical theory of epidemics, part II *Proc. R. Soc.* London, Ser. **A138** (1932) 55–83.

[24] Y. Kuang and E. Beretta, Global qualitative analysis of a ratio-dependent predator-prey systems, *J. Math. Biol.* **36** (1998) 389–406.

[25] Yu. A. Kuznetsov, Elements of applied bifurcation theory, in *Applied. Math. Sci.*, Vol. **112**, Springer-Verlag, New York, 1995.

[26] A. Lajmanovich and J. A. Yorke, A deterministic model for gonorrhea in nonhomogeneous population, *J. Math. Biosci.* **28** (1976) 221–236.

[27] S. A. Levin and D. Pimentel, Selection of intermediate rates of increase in parasite-host systems, *Am. Nat.* **117** (1981) 308–315.

[28] W.-M. Liu, H. W. Hethcote and S. A. Levin, Dynamical behavior of epidemiological models with nonlinear incidence rates, *J. Math. Biol.* **25** (1987) 359–380.

[29] W.-M. Liu, S. A. Levin and Y. Iwasa, Influence of nonlinear incidence rates upon the behavior of SIRS epidemiological models, *J. Math. Biol.* **23** (1986) 187–204.

[30] R. M. May and R. M. Anderson, Possible demographic consequence of HIV/AIDS epidemics: II, assuming HIV infection does not necessarily lead to AIDS, in *Mathematical Approaches to Problems in Resource Management and Epidemiology*, C. Castillo-Chavez, S. A. Levin, and C. A. Shoemaker (eds.), Lecture Notes in Biomathematics **81**, Springer-Verlag, Berlin, 220–248, 1989.

[31] R. Ross, The prevention of malaria, Murry, London, 1911.

[32] S. Run and W. Wang, Dynamical behavior of an epidemic model with nonlinear incidence rate, *J. Differential Equations* **188** (2003) 135–163.

[33] B. Song, C. Castillo-Chavez and J. P. Aparacio, Tuberculosis models with fast and slow dynamics: The role of close and casual contacts, *J. Math. Biosci.* **180** (2002) 187–205.

[34] B. Song, C. Castillo-Chavez and J. P. Aparacio, Global dynamics of tuberculosis model with density dependent demography, in *Mathematical Approaches for Emerging and Reemerging Infectious Diseases: Models, Methods and Theory*, C. Castillo-Chavez with S. Blower, P. van den Driessche, D. Kirschner, and A.-A. Yakubu (eds.), Springer-Verlag, New York, 2002.

[35] B. Song, Dynamical epidemical models and their applications, Cornell University, 2002.

[36] P. van den Driessche and J. Watmough, Reproductive numbers and sub-threshold endemic equilibria for compartment models of disease transmission, *J. Math. Biosci.* **180** (2002) 183–201.

E-mail address: `fsberezo@hotmail.com`
E-mail address: `karev@ncbi.nlm.nih.gov`
E-mail address: `songb@mail.montclair.edu`
E-mail address: `chavez@math.la.asu.edu`